

## Glass powder admixture effect on the dynamic properties of concrete, multi-excitation method

Abdenour Kadik<sup>\*1,2</sup>, Djilali Boutchicha<sup>1</sup>, Abderrahim Bali<sup>2</sup> and Messaouda Cherrak<sup>2</sup>

<sup>1</sup>Laboratory of Applied Mechanics (LMA), University of Science and Technology of Oran, El Mnaouar, BP 1505, Bir El Djir 31000, Oran, Algeria.

<sup>2</sup>Laboratory of civil engineering and environment material (LMGCE),  
Polytechnic School of Algeria – 10 rue Frères Oudek, El-Harrach 16200, Algiers, Algeria

(Received November 20, 2018, Revised June 29, 2019, Accepted January 23, 2020)

**Abstract.** In this work, the dynamic properties of a high performance concrete containing glass powder (GP) was studied. The GP is a new cementitious material obtained by recycling waste glass presenting pozzolanic activity. This eco-friendly material was incorporated in concrete mixes by replacing 20 and 30% of cement. The mechanical properties of building materials highly affect the response of the structure under dynamic actions. First, the resonant vibration frequencies were measured on concrete plate with free boundary conditions after 14, 28 and 90 curing days by using an alternative vibration monitoring technique. This technique measures the average frequencies of several excitations done at different points of the plate. This approach takes into account the heterogeneity of a material like concrete. So, the results should be more precise and reliable. For measuring the bending and torsion resonant frequencies, as well as the damping ratio. The dynamic properties of material such as dynamic elastic modulus and dynamic shear modulus were determined by modelling the plate on the finite element software ANSYS. Also, the instantaneous aroused frequency method and ultrasound method were used to determine the dynamic elastic modulus for comparison purpose, with the results obtained from vibration monitoring technique.

**Keywords:** glass powder; high performance concrete; vibration; resonant frequencies; dynamic properties

### 1. Introduction

Glass powder (GP) is an alternative supplementary Cementitious Material (SCM) which presents a pozzolanic activity (Shayan and xu 2004, Shi *et al.* 2005). This material is obtained by recycling mixed glass, i.e., glass of different colours, which is difficult to recycle because of inherent difficulties in sorting glass by colours. Glass remains in the landfills for a long time because the material does not degrade or decompose. Using GP as an admixture for concrete can contribute to reduce these storage requirements in an eco-friendly and sustainable manner.

A major concern when using glass in concrete is the alkali-silica reaction (ASR). This reaction takes place between the silica, highly abundant in glass, and the alkali present in the pore solution of concrete. The ASR can have a deleterious effect. It is therefore not recommended to use coarse glass or glass fiber without an effective ASR suppressant. However, finely ground glass was found exhibit pozzolanic activity (Shayan, 2002). Shayan and Xu (2004) was among the first to study the replacement of a part of cement by GP. Shayan (2004) concluded that GP can replace up to 30% of cement with satisfactory strength development, a result was confirmed also by Schwarz (2008). The pozzolonic activity of GP increases for finer particles (Shi *et al.* 2005). However, when GP particles are much finer than cement, their strength activity decreases

and the powder turns into a dust (Shi *et al.* 2005). Several studies reported that GP continues to exhibit pozzolanic activity at long time scales, this reaction is thus slow and continuous (Zidol *et al.* 2017, Shayan and Xu 2004, Kamali *et al.* 2015). Also, GP needs enough water to develop the total strength of concrete (Zidol *et al.* 2017). Zidol (2017) concluded that long-term development of compressive strength was more prominent when the water/bender (w/b) ratio was increased in the presence of glass powder.

The GP has also been shown to improve a certain characteristic of durability (Zidol *et al.* 2017, Kamali *et al.* 2015, Schwarz *et al.* 2008). In addition, GP has been used in Ultrahight performance concrete (Soliman and Tagnit-Hamou 2016) because it can reduce hydration heat (Laldji and Tagnit-Hamou 2007). GP has also been incorporated in asphalt concrete for use on roads (Bilondi *et al.* 2016).

Concrete structures can be subjected to impacts, explosions or short forced movements (earthquake). The dynamic response to these actions greatly depends on the compressive strength and elastic constants of the material, i.e., Young's Modulus  $E$  and the Shear modulus  $G$ . These parameters can be determined by the both static and dynamic methods. The dynamic modulus of elasticity is defined as the ratio of stress to strain under vibratory conditions (Lu *et al.* 2013). That is why it is more appropriate to use dynamic parameters to study the structure's vibration both analytically and numerically. Mehta (1986) reported that, the dynamic modulus of elasticity is generally 20, 30, and 40% higher than the static modulus of elasticity for high, medium, and low strength concrete respectively. Also, the elastic constants are affected by the concrete's composition, age, water content and

\*Corresponding author, Ph.D.  
E-mail: [abdn.kadik@gmail.com](mailto:abdn.kadik@gmail.com)

curing conditions (Swamy and Rigby 1971). Besides, some researchers study the relation between dynamic modulus of elasticity and compressive strength (Emiroglu *et al.* 2015).

The static elastic modulus ( $E_s$ ) is generally read off the stress-strain curve obtained from a uniaxial compressive test according to the standard ASTM C469. The dynamic modulus, on the other hand, can be measured using one of the two ways: (1) the resonant frequencies method or (2) the ultrasonic method. Both methods are non-destructive testing (NDT) techniques. The ultrasonic method (Prassianakis 1977, Boumiz *et al.* 1996, Prassianakis 2004) is based on measuring the propagation time of ultrasonic waves in the materials. The resonant frequencies methods use the impact-echo technique or vibration monitoring. The impact-echo method (Pessiki and Carino 1988, Lu *et al.* 2013) measures the short-time response to an impact load according to some predefined standards i.e., ASTM C215. The vibration monitoring technique obtains the fundamental transverse resonant frequency to calculate  $E_d$  has few normalized methods (ASTM C215, DIN 1048 and PN-EN ISO 12680-1). Wang *et al.* (2014) used an impact-echo method on a lumber beam to measure the elastic modulus and validate the results by probabilistic analyses. However, these standards use one point impact excitation which is not really representative of a heterogeneous material like concrete. Several studies (Lu *et al.* 2013, Bahr *et al.* 2013 and Yaogang *et al.* 2015, Emiroglu *et al.* 2015) used a more advanced method using larger specimens and more than one impact excitation point. Here, we present, a vibration monitoring method with multiple impact points.

Damping is an important parameter in vibration structure. It is defined as a dissipation of the mechanical energy on thermal energy. This damping phenomenon is represented by a non-dimensional parameter called a damping ratio. This parameter describes the ability of the material or structure to dissipate vibration energy. However, the total damping of a structure is a complex combination of different damping ability of the elements in the structure: the joints and bearing point, the soil, the material, the beam dimensions and sections. In most cases the material damping is predominant (Swamy and Rigby 1971). Unfortunately, the damping capacity of concrete is poor (Swamy and Rigby 1971). Some admixtures like silica fume and carbon fibres was studied how affect the damping capacity (Ou *et al.* 2006 and 2008, Xu *et al.* 1999). They concluded that this admixture can be employed to enhance the damping capacity of concrete materials. That is why it is important to study the influence of a new admixture on the damping ability of the concrete and study the capacity of such admixture. For example, the value of damping on high performance concrete with a compressive strength between 44-55 MPa is between 0.55 - 0.70% (Giner *et al.* 2011). The higher compressive strength corresponds to the lower damping ratio. This is because the higher compressive strength corresponds to the more compacted one and the more reduced size of pores. This contributes to reduce the internal defect and dislocations of the different interfaces and transition zone, which are responsible for dissipating energy by friction during vibration (Swamy and Rigby 1971).

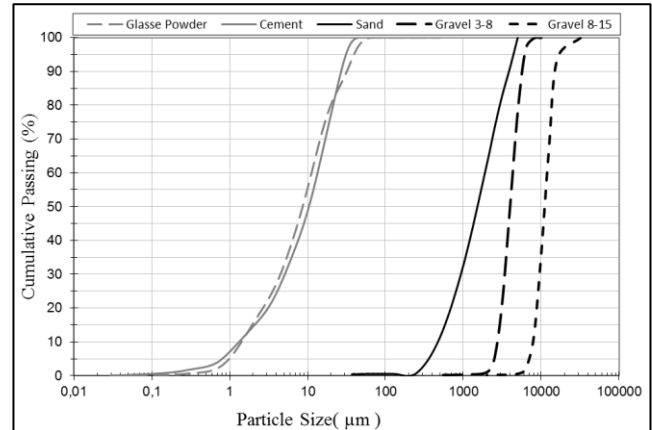


Fig. 1 Particles size distribution of binders and aggregates

Table 1 Chemical composition and physical characteristics of cement and glass powder

Composition (%by mass)/Property	Cement	GP
Loss on ignition	6.89	1.15
Silica (SiO <sub>2</sub> )	18.52	69.86
Alumina (Al <sub>2</sub> O <sub>3</sub> )	4.94	1.75
Iron oxide (Fe <sub>2</sub> O <sub>3</sub> )	3.03	0.54
Calcium oxide (CaO)	0.75	11.80
Magnesium oxide (MgO)	1.97	0.49
Sulfur trioxide (SO <sub>3</sub> )	2.76	0.24
Potassium oxide (K <sub>2</sub> O)	0.66	0.48
Sodium oxide (Na <sub>2</sub> O)	0.11	13.58
Phosphorus oxide (P <sub>2</sub> O <sub>5</sub> )	0.15	0.02
Titanium oxide (TiO <sub>2</sub> )	0.24	0.10
Specific surface area (m <sup>2</sup> /kg)	361	452
Density (kg/m <sup>3</sup> )	3100	2500

## Research significant

The main objective of the present work is to study the influence of the GP substitution to cement on the mechanical properties of concrete, focusing on its dynamic properties and damping ratio. Also, this study aims to evaluate the reliability and precision of the results obtained by multi-excitation method for measuring vibration frequencies of a shape and the dynamic properties of a material.

## 2. Materials and test methods

### 2.1 Materials and specimen preparation

We used CPJ-CEM II / A 52.5 Portland cement, produced according to local standard (NA 442, 2013). Silica fume based on micro silica (composed of 85% SiO<sub>2</sub>) was

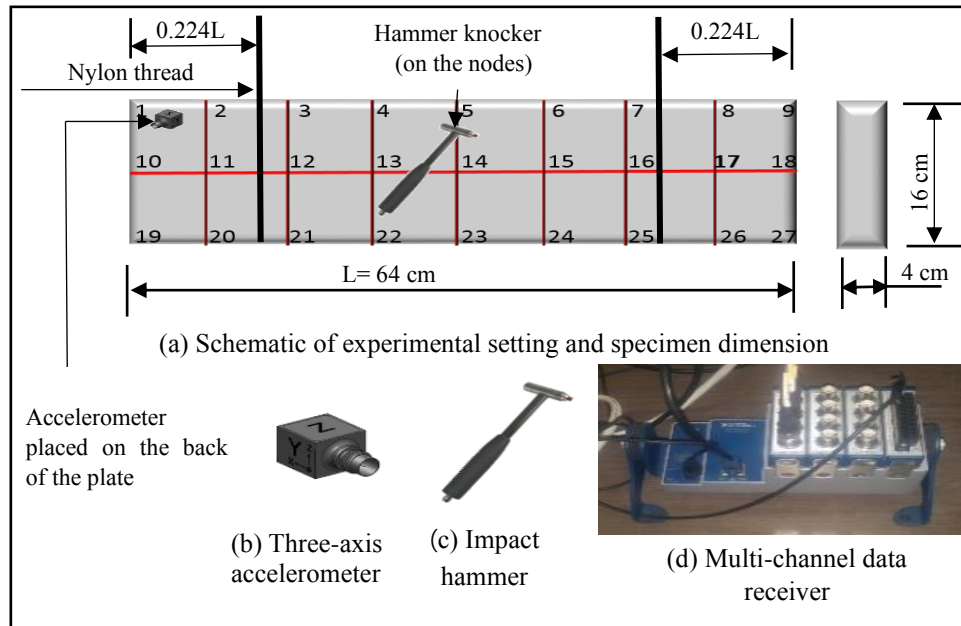


Fig. 2 schematic of experimental setting and experimental devices for free vibration test

used as an additive. A 0-5mm sand and two gravel classes 3-8mm and 8-15mm were used for the aggregates.

The glass powder (GP) was obtained from recycling differently coloured glass bottles. They were collected, cleaned, and then crushed to be dried in an oven at 105°C. After removing the fines by sieving and taking only elements bigger than 3 mm, the glass was ground in the laboratory using electrical grinding balls with 10 kg capacity. The grinding sequence consisted of six grindings of 25 minutes, each separated by a rest period of 10 to 15 minutes.

The chemical composition and physical characteristics of GP and cement used are shown on Table 1. Also, the size distribution of GP, cement and aggregates are shown on the fig. 1.

In the first, the reference concrete mix was formulated with water to binder (w/b) ratio of 0.3. Then, three types of concrete mixes were prepared: (1) the reference concrete specimen, denoted as HPC, (2) mix with 20% of cement replacement, denoted as HPC-20GP, (3) mix with 30% of cement replacement, denoted as HPC-30GP. The rates of substitution were chosen to be the maximum without any notable decrease in strength of the concrete (Shayan and xu 2004, Schwarz *et al.* 2008). The contents of these different mixes are reported on Table 2.

Nine cubic and nine prismatic specimens were cast for each of the three concrete mixtures. After 24 hours, all the specimens were released from the moulds and cured in water. Three specimens' type of each mixture were tested after 7, 28 and 90 days. The cubic specimens (100x100x100 mm) were used in compression tests following standard NF EN 12390(2012). Prismatic specimens (280x700x700 mm) were used in three-point flexural tests to measure the mixture's tensile strength according to standard NF EN 14651 (2007).

Three concrete plates (640x160x40 mm) were used for the vibration tests which were carried out after curing in water for 14, 28 and 90 days.

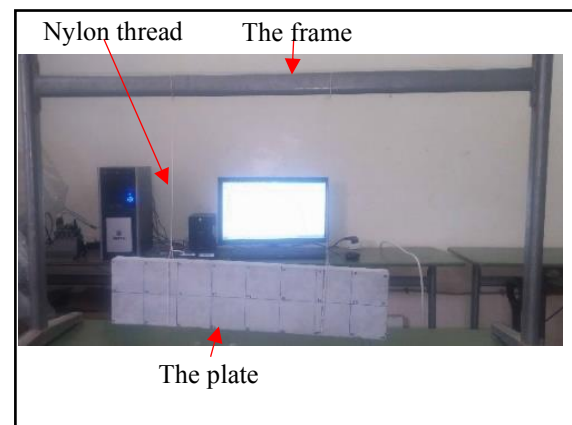


Fig. 3 experimental setting for free vibration test.

## 2.2 Dynamic testing method

The frequency measurements on the plates were carried out using a PCB PIEZOTRONICS device from National Instruments Company. The device (Fig. 2) consists of the following:

- One triaxial accelerometer, PCB Model 356A15 with a high sensitivity of 10.2 mV/(m/s<sup>2</sup>) ( $\pm 10\%$ ), made of titanium with ceramic sensing element.
- One impact hammer, PCB Model 086C03 with sensitivity of 2.25 mV/N ( $\pm 15\%$ ), made of quartz sensing element.
- The multi-channel data receiver, Model National Instrument 9234 CompactDAQ, used to receive and amplify the signal
- A signal processing software called SO Analyzer of m+p International.

Sixteen meshes with 27 nodes numbered from 1 to 27 were drawn on each plate (Fig. 2(a)). The plate was suspended from a frame on Nylon threads attached on each

Table 2 Mix proportions of 1 m3 of mixes and hard properties of the concrete

	Kg/m <sup>3</sup>								%	
	C	GP	SF	S	G 3/8	G8/15	W	SP (2%)	Density	Porosity
HPC	420	-	33.6	610	454.5	565.5	136	30.24	2451	4.82
HPC-20GP	336	84	33.6	610	454.5	565.5	136	30.24	2462	4.43
HPC-30GP	294	126	33.6	610	454.5	565.5	136	30.24	2490	4.37
	C cement,	GP Glass Powder,	SF Silica Fume,	S Sand,	G Gravel,	W Water,	SP Superplasticizer			

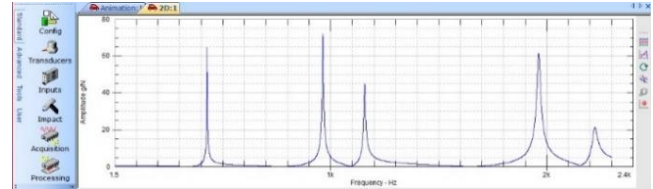
side of the plate (fig. 2(a) and 3). The nylon bands were attached at those locations correspond to the theoretical nodes' lines of the first-order bending vibration mode, i.e., at a distance of  $0.024L$  ( $L=64\text{cm}$ ) from the edge. The accelerometer was placed on the back of the plate, at the same axe of the node number 1 to have the furthest measurement point from the impact of the hammer, i.e., Knock at the node number 27 is the diagonal furthest point from the recording. The accelerometer was connected to a multi-channel data receiver to amplify the signal. The graphical representation of the plate was drawn using the SO Analyzer software, replication the same meshes and nodes numbers. An individual excitation was produced by gently impacting the plate on the 27 nodes by the hammer, running through all 27 points sequentially. The impacts order follows the indication given by the SO Analyzer software. The signals were treated using a multi-channel data receiver and SO Analyzer software recording the signals given by the hammer and the accelerometer over time to be transformed into the frequency domain using a Fast Fourier Transform (FFT). The SO Analyzer software produced a series of frequency response functions (FRF) (Fig. 4(a)) and showing the frequencies of the different vibration modes. The SO Analyzer software treat the 27 FRF provided of each excitation and gives the average FRF of the plate. The software also provided the shape of the vibration modes (Fig. 4(b), and the damping ratio of each mode.

### 2.3 Dynamic elastic constants

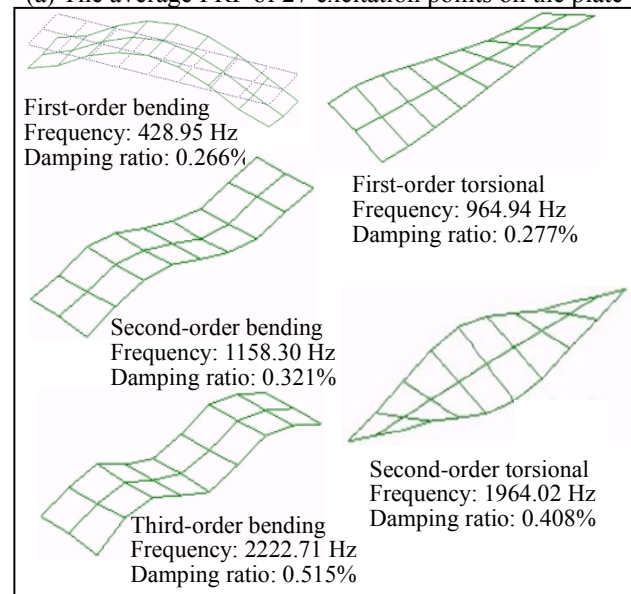
The finite element software ANSYS has been used for modelling the experimental plate assuming a free boundary condition. The meshed model is represented in fig. 4(C). The frequencies and the shapes of the free resonant vibrations can be determined by the ANSYS model. The first and the second frequencies of resonant vibration are a bending mode and a torsional mode respectively. By varying the material properties: elastic modulus ( $E$ ) and Poisson ratio ( $\nu$ ), the frequency of the first and second mode of vibration obtained from the model can be adapted to match those obtained experimentally. Therefore, we obtain the dynamic modulus "of elasticity ( $E_{dv}$ ) and the Poisson coefficient ( $\nu$ ). However, the dynamic shear modulus ( $G_{dv}$ ) is given by eq. (1).

$$G_{dv} = \frac{E_{dv}}{2(1 + \nu)} \quad (1)$$

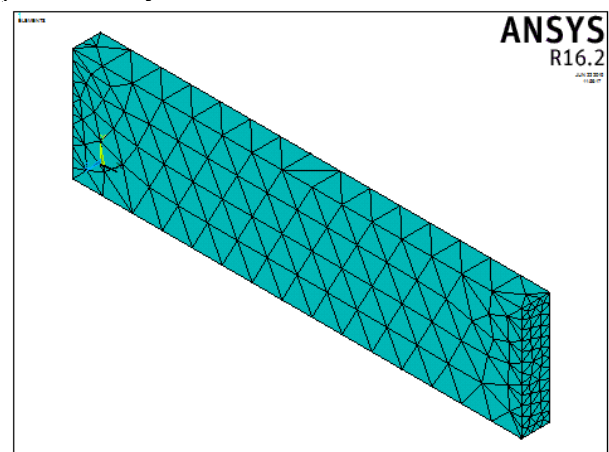
Wang *et al.* (2015) research, using an experimental method similar to ours, validated analytically that the dynamic parameters: elastic modulus  $E$ , shear modulus  $G$



(a) The average FRF of 27 excitation points on the plate



(b) The shapes of the resonant vibration modes – HPC plate at 90 days



(c) The meshed plate modelled in ANSYS software  
Fig. 4 Results given by SO Analyze Software and ANSYS of free vibration test on the plate

and Poisson ratio  $\nu$  for the concrete, follow the relationship given by Eq. (1).

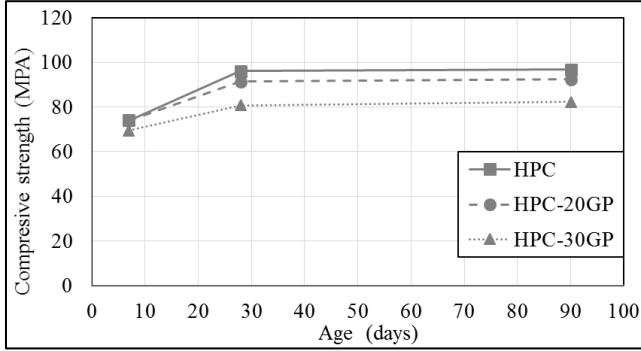


Fig. 5 Evolution of compressive strength of different mixtures

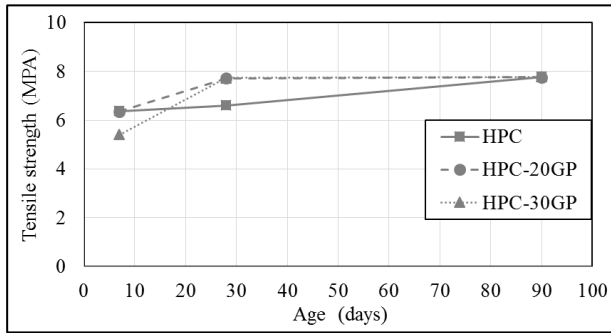


Fig. 6 Evolution of tensile strength of different mixtures

#### 2.4 Elastic modulus by instantaneous aroused frequency method

According to the transverse bending theory, for an Euler Beam, the elastic modulus can be determined by the natural frequency of the first bending mode of a free beam (Cheng and Timesheko 1965), eq. (2).

$$2\pi f_1 = (4.730041)^2 \sqrt{\frac{EI}{\rho AL^4}} \quad (2)$$

where  $f_1$  the first bending frequency (Hz),  $E$  is the elastic modulus of the beam,  $I$  and  $A$  are the inertia and area of the section respectively,  $\rho$  is the air-dry density of the beam.

For rectangular section, the Elastic modulus can be drawn in Eq. (3)

$$E_f = 0.9462 \frac{\rho f_1^2 L^4}{h^2} \quad (3)$$

where  $E_f$  is the Elastic modulus of the beam (Pa),  $\rho$  is the air-dry density ( $\text{kg/m}^3$ ),  $f_1$  is the first bending frequency (Hz),  $L$  is the length of the tested beam,  $h$  is the high of the tested beam.

This method was used for lumber beam by Wang *et al.* (2014). The probabilistic analyses confirm that the results of such a method are relevant.

#### 2.5 Elastic modulus by Ultrasonic method

We used a second method to determine the dynamic elastic modulus ( $E_d$ ) and then compared it to the result obtained using the vibration method. The propagation

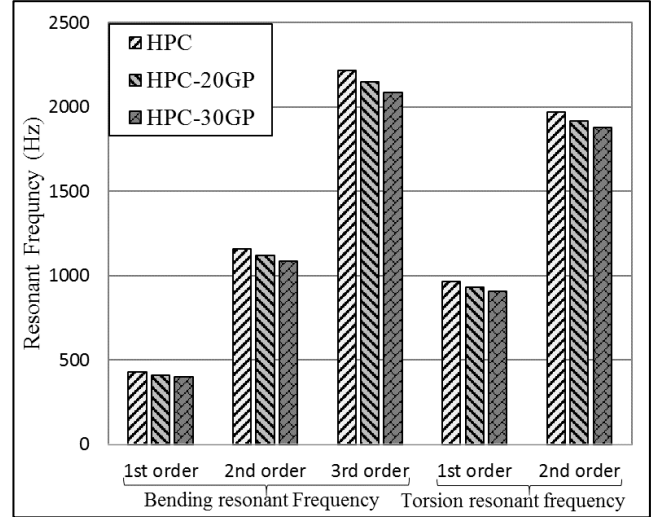


Fig. 7 Resonant frequencies modes of different mixes

velocity of the ultrasonic waves in a section of concrete depends on the density of the material and the elastic modulus (Prassianakis 1977 and 2004). By measuring this velocity, we can determine the dynamic elastic modulus  $E_{ds}$ . So,  $E_{ds}$  can be determined by the eq. (4) (Prassianakis 1977 and 2004):

$$E_{ds} = \frac{(1 + \nu)(1 - 2\nu)}{(1 - \nu)} \gamma V^2 \quad (4)$$

where  $\gamma$  is the concrete's density,  $\nu$  is the Poisson coefficient and  $V$  is the sound velocity.

### 3. Results and discussion

#### 3.1 Concrete strength

##### 3.1.1 Compressive strength

The compressive strength at various curing ages is shown in Fig. 5. According to the results, the compressive strength of the mixes reached values ranging between 82-97 MPa. It can be seen that the substitution of a part of cement by GP led to a slight decrease in the compressive strength at all curing ages. The differences appear proportional to the GP percentage replacement. After 90 days, the HPC-20GP and HPC-30GP mixtures exhibited 95.1% and 84% of the compressive strength of the control mix (HPC), respectively. It should be noted that the strength increased between day 28 and 90 is 0.6%, 1.1 % and 1.8% for the HPC, HPC-20GP and HPC-30GP mixtures, respectively. The development of strength after day 28 is more important for the concrete containing glass powder because of the pozzolanic activity of GP is slow but continuous (Zidol *et al.* 2017, Shayan and Xu 2004).

##### 3.1.2 Tensile strength

Fig. 6 shows the evolution of the tensile strength of the mixtures. At 28 curing days, the tensile strength of concrete with GP is higher than the reference concrete (HPC). However, the tensile strengths achieved after 90 curing days

Table 3 Values of bending and torsional frequencies vibration of the plate the differences between experimental and modelling values ( $F_{EX}-F_M$ )

SD: Standard deviation of the three specimens tested			$F_{EX}-F_M$ : difference between the experimental and modelling values					
	Bending resonant frequencies			Torsion resonant frequencies				
	1st order (Hz $\pm$ SD)	2nd order (Hz $\pm$ SD)	$F_{EX}-F_M$ (%)	3rd Order (Hz $\pm$ SD)	$F_{EX}-F_M$ (%)	1st order (Hz $\pm$ SD)	2nd order (Hz $\pm$ SD)	$F_{EX}-F_M$ (%)
90 Days								
HPC	428.66 $\pm$ 2.31	1159.81 $\pm$ 1.13	0,44	2218.75 $\pm$ 5.58	0,6	966.52 $\pm$ 4.12	1971 $\pm$ 6.70	0,26
HPC-20GP	410.44 $\pm$ 4.12	1121.58 $\pm$ 10.91	1,16	2151.39 $\pm$ 17.44	1,85	929.43 $\pm$ 8.93	1917.88 $\pm$ 16.92	1,1
HPC-30GP	400.79 $\pm$ 3.39	1084.66 $\pm$ 8.82	1,4	2087.69 $\pm$ 11.77	1,42	908.65 $\pm$ 9.39	1877.25 $\pm$ 18.49	1,21
28 Days								
HPC	426.57 $\pm$ 2.30	1155.63 $\pm$ 1.24	0,35	2205.22 $\pm$ 4.80	0,48	963.26 $\pm$ 3.96	1960.98 $\pm$ 3.08	0,44
HPC-20GP	406.76 $\pm$ 4.24	1112.26 $\pm$ 12.03	1,25	2136.48 $\pm$ 18.21	2,079	923.87 $\pm$ 8.81	1909.98 $\pm$ 15.64	1,3
HPC-30GP	393.27 $\pm$ 2.53	1071.37 $\pm$ 2.44	0,88	2063.47 $\pm$ 8.42	1,96	899.88 $\pm$ 6.64	1859.01 $\pm$ 15.60	1,26
14 Days								
HPC	424.89 $\pm$ 2.57	1149.95 $\pm$ 5.14	0,48	2199.95 $\pm$ 4.70	0,55	959.4 $\pm$ 5.50	1956.97 $\pm$ 5.17	0,5
HPC-20GP	397.78 $\pm$ 7.67	1088.19 $\pm$ 21.66	1,35	2093.85 $\pm$ 35.89	1,97	1242.39 $\pm$ 8.46	1887.85 $\pm$ 26.86	1,02
HPC-30GP	386.39 $\pm$ 2.56	1054.55 $\pm$ 0.36	0,83	2037.36 $\pm$ 7.77	1,33	890.17 $\pm$ 8.78	1842.18 $\pm$ 14.43	1,12

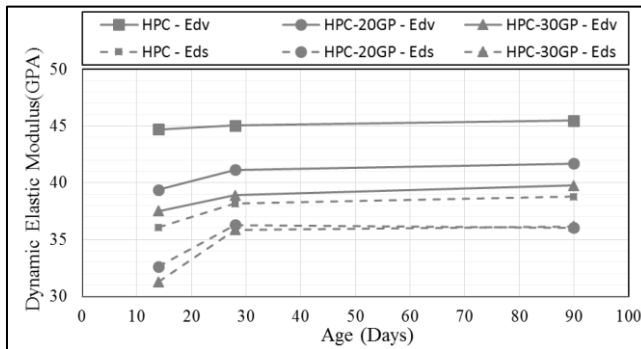


Fig. 8 Evolution of Elastic modulus of mixes determined by vibration method (Edv) and ultrasonic method (Eds)

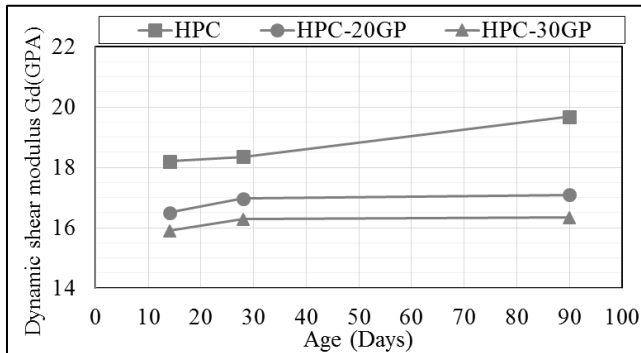


Fig. 9 Evolution of dynamic shear modulus of mixes

are approximately the same for all mixes, about 7.8 MPa. This same tensile strength development of different mixtures at long term is due to the little differences in compressive strength.

### 3.2 Dynamic properties

#### 3.2.1 Resonant frequencies

Fig. 4(a) shows the overall average of 27 frequency spectra (FRF) resulting from 27 individual excitations at the plate's node points. Each frequency peak corresponds to a resonant vibration frequency. Fig. 4(b) shows the shape of

Table 5 Values of damping ratio of mixes after 90 days

Motion	Damping ratio (%)		
	HPC	HPC-20GP	HPC-30GP
Bending	0,275 $\pm$ 0.028	0,305 $\pm$ 0.025	0,379 $\pm$ 0.013
Torsion	0,324 $\pm$ 0.033	0,260 $\pm$ 0.012	0,295 $\pm$ 0.014

the resonant vibration mode as obtained from SO Analyzer software. The first, third, and fifth frequencies correspond to a bending mode, whereas the second and fourth frequencies correspond to torsion vibration modes.

Table 3 and fig. 7 shows the average values on three plate specimens of the five first resonant frequencies obtained at 14, 28 and 90 days. The first resonant frequencies between 350-430 Hz correspond to the first longitudinal bending vibration mode. The third (960-1160Hz) and fifth (1680-2220Hz) resonant frequencies correspond to the second and third bending vibration modes, respectively. The second and fourth resonant frequencies fit the first and second torsion vibration modes with 810-970Hz and 1390-1980Hz, respectively. Replacing up to 30% of the cement by GP reduces the resonant vibration frequencies (Fig. 7) proportionally to the amount of cement replacement. The frequencies are reduced by 2 to 4% for HPC-20GP and by 4.5 to 6.5% for HPC-30GP.

The comparison of the five vibration modes frequencies obtained from experiments ( $F_{EX}$ ) to the results obtained from the model simulations ( $F_M$ ) are denoted  $F_{EX}-F_M$  (Tab. 3). There are no differences ( $F_{EX}-F_M$ ) in the first bending and first torsional vibration frequencies modes because we make it to be equals in determining the material characteristics. We note that the differences for the bending modes do not exceed 2.7% for all mixes and curing ages. Also, for the resonant torsion frequencies, the differences do not exceed 1.6%. Therefore, we can conclude that this method of determining the elastic modulus properties is both reliable and precise. In addition, the standard deviations are generally around 1% and do not exceed 2% for all mixes which strength this conclusion.

Table 4 Values of elastic constants by vibration method and elastic modulus by ultrasonic method

SD: Standard deviation of the three specimens tested					
	Vibration method			Frequency method	Ultrasonic method
	Elastic Modulus $E_d$ (GPa $\pm$ SD)	Shear modulus $G_d$ (GPa $\pm$ SD)	Poisson ratio $\mu$	Elastic Modulus $E_f$ (GPa $\pm$ SD)	Elastic Modulus $E_{ds}$ (GPa $\pm$ SD)
90 Days					
HPC	45.47 $\pm$ 0.50	18.48 $\pm$ 0.15	0.230 $\pm$ 0.005	44.68 $\pm$ 0.59	38.77 $\pm$ 0.23
HPC-20GP	41.70 $\pm$ 0.84	17.09 $\pm$ 0.33	0.220 $\pm$ 0.003	41.15 $\pm$ 1.01	36.04 $\pm$ 0.37
HPC-30GP	39.75 $\pm$ 0.67	16.34 $\pm$ 0.35	0.217 $\pm$ 0.030	39.69 $\pm$ 0.82	36.15 $\pm$ 0.22
28 Days					
HPC	45.04 $\pm$ 0.48	18.36 $\pm$ 0.15	0.227 $\pm$ 0.006	44.55 $\pm$ 0.82	38.16 $\pm$ 0.40
HPC-20GP	41.13 $\pm$ 0.86	16.97 $\pm$ 0.32	0.212 $\pm$ 0.002	40.51 $\pm$ 1.10	36.28 $\pm$ 0.37
HPC-30GP	38.90 $\pm$ 0.50	16.29 $\pm$ 0.24	0.194 $\pm$ 0.006	37.87 $\pm$ 0.88	35.86 $\pm$ 0.64
14 Days					
HPC	44.70 $\pm$ 0.63	18.20 $\pm$ 0.21	0.227 $\pm$ 0.005	44.20 $\pm$ 0.97	36.06 $\pm$ 0.47
HPC-20GP	39.40 $\pm$ 0.15	16.50 $\pm$ 0.41	0.191 $\pm$ 0.018	38.75 $\pm$ 1.66	32.62 $\pm$ 0.56
HPC-30GP	37.50 $\pm$ 0.50	15.90 $\pm$ 0.32	0.178 $\pm$ 0.020	36.55 $\pm$ 0.62	31.30 $\pm$ 0.28

### 3.2.2 Dynamic elastic properties

The values of the dynamic elastic modulus obtained by different methods at 14, 28 and 90 days are given in Table 4 and illustrated in Fig. 8. According to the results, the  $E_{dv}$  of the mixes reached values between 39.5 and 45.5 GPa. GP substitution of part of the cement led to a slight decrease in  $E_{dv}$  at all curing ages proportionally to the amount of GP replacement. At 90 days, the mixture HPC-20GP showed a decrease of 8.3% compared with the control mix HPC, while HPC-30GP had a 12.6% low value.

The values of dynamic elastic modulus obtained by instantaneous aroused frequency method reported in the table 4 are really close to those obtained by vibration method. All the values are lower to the dynamic values. However, the difference does not exceed 1.75%.

The dynamic elastic modulus obtained by the ultrasonic method ( $E_{ds}$ ) at 14, 28 and 90 days are given in Table 4 and plotted in Fig. 9.  $E_{ds}$  values show the same evolution pattern through curing age as the values obtained from the vibration method but the absolute values are 10% to 15% lower in comparison.

The values of dynamic shear modulus  $G_{dv}$  obtained after 14, 28 and 90 days of curing are presented in Table 4 and illustrated in Fig. 9. The maximum shear modulus is obtained for the HPC, control mixture, with 19.69 GPa. The concrete with GP shows a reduction in the shear modulus, decrease of 13.2% for the HPC-20GP and 17% for the HPC-30GP after 90 days of curing.

For the Poisson coefficient, the same pattern can be observed as for the elastic and shear modulus (fig. 10). It is maximal for HPC with a value of 0.23. For HPC-20GP and HPC-30GP the poison coefficients are 4.3% and 5.6% lower than the HPC value, respectively.

### 3.2.3 Damping ratio

The values of the damping ratio for different mixtures obtained after 90 days of curing are given in Table 5. The damping ratio presented in this table concern the first resonant bending mode, called bending damping, and the first resonant torsion mode, called torsion damping.

The values of bending damping are between 0.275 and 0.38%. The control mix, without GP, showed the lowest

ratio (0.275%), while HPC-20GP and HPC-30GP had ratios of 0.305% and 0.379%, respectively. This is due to the ability of the material to dissipate vibration energy and is directly related to the structure of the material. More compact concretes with reduced size pores, have less important damping ratio (Giner *et al.* 2011). In this study the concrete with GP have a more compact concrete (density mass of 2462 kg/m<sup>3</sup> and 2490 kg/m<sup>3</sup>) and less pore size (4.43 and 4.37%) for respectively HPC-20GP and HPC-30GP (tab. 2) compared with the reference concrete (density of 2451 kg/m<sup>3</sup> and porosity of 4.82%). That is why the higher the compressive strength the lower the bending damping ratio. Giner (2011) concluded that this behavior is due to internal defects and dislocations of the different interfaces and transition zone which are responsible for dissipating energy through friction during vibration. The damping torsion ratio are lower for the mixes with GP and its values are between 0.29 and 0.33%.

## 4. Conclusion

The aim of this work was to investigate the influence of replacement part of the cement with GP on both the dynamic and static mechanical properties of high performance concrete. From the results obtained, the following conclusions can be drawn:

- Replacing 20 to 30% of cement by GP reduces the compressive strength of the concrete by 4 and 15% but does not affect the tensile strength at long time period.
- The resonant frequencies of concrete specimens slightly decreased for mixes containing GP.
- The elastic modulus obtained using a vibration technique is between 10 and 15% higher compared to values obtained through an ultrasound method.
- The dynamic elastic constants, elastic and shear modulus, decrease with increasing GP content.
- This measurement proved to be reliable and precise because there were no significant differences between experimental and modelling results beyond the second resonant frequencies. Furthermore, there is only minor differences of the frequencies for the same mix (based on



standard deviations) which proved the repetitively of the experience.

## Acknowledgments

I would like to express my gratitude to Professor SEREIR Zouaoui, Director of the Laboratory of Composite Structures and Innovative Materials at Oran University (USTO-MB) in Algeria, for having made available to me computer resources for numerical simulations with ANSYS.

## References

- ASTM C215 (2002), Standard Test Method for Fundamental Transverse, Longitudinal, and Torsional Resonant Frequencies of Concrete Specimens, ASTM, PA, USA.
- ASTM C 469(2000), *Test Method for Static Modulus of Elasticity and Poisson's Ratio of Concrete in Compression*, Annual Book of ASTM Standards, PA, USA.
- Bahr, O., Schaumann, P., Bollen, B. and Bracke, J. (2013), "Young's modulus and Poisson's ratio of concrete at high temperatures: Experimental investigations", *Mater. Design*, **45**, 421-429.
- Bilondi, M.P., Marandi, S.M. and Ghasemi, F., "Effect of recycled glass powder on the asphalt concrete modification", *Struct. Eng. Mech.*, **59**, 373-385. <https://doi.org/10.1016/j.matdes.2012.07.070>.
- Boumiz, A., Vernet, C. and Tenoudji F.C. (1996), "Mechanical properties of cement pastes and mortars at early ages: evolution with time and degree of hydration", *Adv. Cement Based Mater.*, **3**, 94-106. [https://doi.org/10.1016/S1065-7355\(96\)90042-5](https://doi.org/10.1016/S1065-7355(96)90042-5).
- Cheng, K., and Timoshenko, S. (1965). *Textbook of Mechanical Vibrational Science*, Technical Industry Press, Beijing.
- DIN 1048 (1991), *Prüfung von Beton, Empfehlungen und Hinweise als Ergänzung zu*, Deutscher Ausschuss für Stahlbeton, Berlin (in German).
- Emiroglu, M., Yildiz, S., Kelestemur, M.H. (2015), "A study on dynamic modulus of self-consolidating rubberized concrete", *Struct. Eng. Mech.*, **15**(5), 795-805. <https://doi.org/10.12989/cac.2015.15.5.795>.
- Giner, V.T., Ivorra, S., Baeza, F.J., Zornoza, E., Ferrer, B. (2011), "Silica fume admixture effect on the dynamic properties of concrete", *Construct. Build. Mater.*, **25**, 3272-3277. <https://doi.org/10.1016/j.conbuildmat.2011.03.014>.
- Kamali, M. and Ghahremaninezhad, A. (2015), "Effect of glass powders on the mechanical and durability properties of cementitious materials", *Construct. Build. Mater.*, **10**, 407-416. <https://doi.org/10.1016/j.conbuildmat.2015.06.010>.
- Laldji, S. and Tagnit-Hamou, A. (2007), "Glass frit for concrete structures: a new, alternative cementitious material", *Can. J. Civ. Eng.*, **34**, 793-802. <https://doi.org/10.1139/l06-168>.
- Lu, X., Sun, Q., Feng, W. and Tian, J. (2013), "Evaluation of dynamic modulus of elasticity of concrete using impact-echo method", *Construct. Build. Mater.*, **47**, 231-239. <https://doi.org/10.1016/j.conbuildmat.2013.04.043>.
- MEHTA, P.K. (1986), *Concrete Structure Properties and Materials*, Englewood Cliffs, New Jersey.
- NA442/2013 "Ciment - composition, spécification et critères de conformité des ciments courants", Institut Algérien de Normalisation (IANOR), 21.
- NF EN 12390 (2012), "Essai pour le béton durci – Partie 3: résistance à la compression des éprouvettes", Association Française de normalisation (AFNOR).
- NF EN 14651 (2007), "Méthode d'essai du béton de fibres métalliques – Mesurage de la résistance à la traction par flexion (limite de proportionnalité (LOP), résistance résiduelle)", Association Française de normalisation (AFNOR).
- Ou, J.P., Liu, T.J. and Li, J.H. (2006), "Analysis of the damping behavior and microstructure of cement matrix with silane-treated silica fume", *J. Wuhan Univ. Technol. Mater. Sci.*, **21**(2), 1-5. <https://doi.org/10.1007/BF02840826>.
- Ou, J.P., Liu, T.J., Li, J.L., (2008), "Dynamic and seismic property experiments of high damping concrete and its frame models", *J. Wuhan Univ. Technol. Mater. Sci. Ed.*, **23**(2), 1-6.
- Pessiki, S.P. and Carino, N.J. (1988), "Setting time and strength to concrete using the impact-echo method", *ACI Materials J.*, **85**, 389-399.
- Prassianakis, I.N. (1977), "Moduli of elasticity evaluation using ultrasound", *Insight*, **39**, 425-429.
- Prassianakis, I.N. (2004), "Ultrasonic testing of non-metallic materials: concrete and marble", *Theoretical Appl. Fracture Mech.*, **42**, 191-198.
- PN-EN ISO 12680-1(2008), "Methods of test for refractory products -- Part 1: Determination of dynamic Young's modulus (MOE) by impulse excitation of vibration", ISO.
- Schwarz, N., Cam, H and Neithalath, N. (2008), "Influence of fine glass powder on the durability characteristics of concrete and its comparison to fly ash", *Cement Concrete Compos.*, **30**, 486-496.
- Shayan, A. (2002), "Value-added utilisation of waste glass in concrete", IABSE Symposium Melbourne, Melbourne, September.
- Shayane, A. and Xu, A. (2004), "Value-added utilisation of waste glass in concrete", *Cement Concrete Res.*, **34**, 81-89. [https://doi.org/10.1016/S0008-8846\(03\)00251-5](https://doi.org/10.1016/S0008-8846(03)00251-5).
- Shi, C., Wu, Y., Riefler, C. and Wang, H. (2005), "Characteristics and pozzolanic reactivity of glass powders", *Cement Concrete Res.*, **35**, 987-993. <https://doi.org/10.1016/j.cemconres.2004.05.015>.
- Soliman, N.A. and Tagnit-Hamou, A. (2016), "Development of ultra-high- performance concrete using glass powder – Towards ecofriendly concrete", *Construct. Build. Mater.*, **125**, 600-612. <https://doi.org/10.1016/j.conbuildmat.2016.08.073>.
- Swamy, N. and Rigby G. (1971), "Dynamic properties of hardened paste, mortar and concrete", *Mater. Struct.*, **4**(1), 13-40. <https://doi.org/10.1007/BF02473927>.
- Wang, Z., Gao, Z., Wang, Y., Cao, Y., Wang, G., Liu, B. and Wang, Z., (2015), "A new dynamic testing method for elastic, shear modulus and Poisson's ratio of concrete", *Construct. Build. Mater.*, **100**, 129-135. <https://doi.org/10.1016/j.conbuildmat.2015.09.060>.
- Xu, Y. and Chung, D.D.L., "Effect of carbon fibers on the vibration-reduction ability of cement", *Cem. Concr. Res.*, **29**, 1107-1109. [https://doi.org/10.1016/S0008-8846\(99\)00078-2](https://doi.org/10.1016/S0008-8846(99)00078-2).
- Yaogang, T., Shuaifeng, S., Kan, J. and Shuguang, H. (2015), "Mechanical and dynamic properties of high strength concrete modified with lightweight aggregates presaturated polymer emulsion", *Construct. Build. Mater.*, **93**, 1151-1156. <https://doi.org/10.1016/j.conbuildmat.2015.05.015>.
- Wang, Z., Wang, Z., Wang, B. J., Wang, Y., Liu, B., Rao, X., Wel, P. and Yang, Y. (2014), "Dynamic testing and Evaluation of Modulus of Elasticity (MOE) of SPF Dimensional Lumber", *BioResources*, **9**(3), 3869-3882.
- Zidol, A., Tognonvi, M.T. and Tagnit-Hamou, A. (2017), "Effect of Glass Powder on Concrete Sustainability", *New J. Glass Ceramics*, **7**, 34-47.